Mice Lacking *bi-1* Gene Show Accelerated Liver Regeneration

Béatrice Bailly-Maitre,[1] Emilie Bard-Chapeau,[1] Fréderic Luciano,[1] Nathalie Droin,[2] Jean-Marie Bruey,[1] Benjamin Faustin,[1] Christina Kress,[1] Juan M. Zapata,[1] and John C. Reed[1]

[1]Burnham Institute for Medical Research, La Jolla, California and [2]La Jolla Institute for Allergy and Immunology, Division of Cellular Immunology, San Diego, California

Abstract

The liver has enormous regenerative capacity such that, after partial hepatectomy, hepatocytes rapidly replicate to restore liver mass, thus providing a context for studying *in vivo* mechanisms of cell growth regulation. Bax inhibitor-1 (BI-1) is an evolutionarily conserved endoplasmic reticulum (ER) protein that suppresses cell death. Interestingly, the BI-1 protein has been shown to regulate Ca^{2+} handling by the ER similar to antiapoptotic Bcl-2 family proteins. Effects on cell cycle entry by Bcl-2 family proteins have been described, prompting us to explore whether *bi-1*–deficient mice display alterations in the *in vivo* regulation of cell cycle entry using a model of liver regeneration. Accordingly, we compared *bi-1*$^{+/+}$ and *bi-1*$^{-/-}$ mice subjected to partial hepatectomy with respect to the kinetics of liver regeneration and molecular events associated with hepatocyte proliferation. We found that *bi-1* deficiency accelerates liver regeneration after partial hepatectomy. Regenerating hepatocytes in *bi-1*$^{-/-}$ mice enter cell cycle faster, as documented by more rapid incorporation of deoxynucleotides, associated with earlier increases in cyclin D1, cyclin D3, cyclin-dependent kinase (Cdk) 2, and Cdk4 protein levels, more rapid hyperphosphorylation of retinoblastoma protein, and faster degradation of $p27^{Kip1}$. Dephosphorylation and nuclear translocation of nuclear factor of activated T cells 1 (NFAT1), a substrate of the Ca^{2+}-sensitive phosphatase calcineurin, were also accelerated following partial hepatectomy in BI-1–deficient hepatocytes. These findings therefore reveal additional similarities between BI-1 and Bcl-2 family proteins, showing a role for BI-1 in regulating cell proliferation *in vivo*, in addition to its previously described actions as a regulator of cell survival. [Cancer Res 2007;67(4):1442–50]

Introduction

In mammals, the liver is noteworthy in its ability to rapidly regenerate in response to massive cellular injury from toxic exposure, viral infections, or surgical resection. In rodent models, liver mass is restored to normal within 2 to 3 days after surgical excision of two thirds of the organ (1, 2). The rapid regrowth of the liver thus provides a robust *in vivo* model for studying cell cycle entry and cell proliferation. The remarkable regenerative capacity of the liver may also predispose this organ to carcinogenesis. Annually, more than a half million persons die of hepatocellular carcinoma (3).

Liver regeneration after partial hepatectomy is a tightly regulated process that proceeds through distinct stages, including withdrawal of hepatocytes from quiescence ("priming"), cell cycle entry and progression, several rounds of cell division, and finally cessation of cell division and return of hepatocytes to quiescence, in concert with tissue remodeling to restore normal hepatic architecture (4, 5). The molecular signals triggering liver regeneration are thought to include cytokines, growth factors, reactive oxygen species, complement factors C3 and C5 (6), and possibly bacterial lipopolysaccharide (1, 2) released into the portal circulation. Gene ablation studies in mice show that interleukin (IL)-6 and tumor necrosis factor-α (TNF-α) are important contributors to liver regeneration (7, 8), and some of their immediate downstream transcription factors have been identified as crucial regulators of the regenerative process, including signal transducers and activators of transcription 3 (STAT3), nuclear factor-κB (NF-κB), activator protein-1, and c-Myc (4, 9). As in all eukaryotic cells, cycle progression of activated hepatocytes is regulated by the activity of complexes consisting of cyclins and cyclin-dependent kinases (Cdk). These kinase complexes function in a coordinated manner to phosphorylate the retinoblastoma protein (Rb) and related proteins, thereby releasing bound E2F transcription factors required for G_1 to S transition (9).

Recently, the antiapoptotic protein Bax inhibitor-1 (BI-1) has been recognized as a regulator of apoptosis linked to endoplasmic reticulum (ER) stress (10). BI-1 contains several transmembrane domains, localizes to ER membranes, and has cytoprotective functions that are conserved in both animal and plant species (11). BI-1 protein suppresses apoptosis induced by ectopic expression of proapoptotic protein Bax as well as selected other types of stimuli. Cells from BI-1 knockout (KO) mice, including hepatocytes, display selective hypersensitivity to apoptosis induced by ER stress–causing chemical agents (thapsigargin, tunicamycin, and brefeldin A) or by ischemia-reperfusion (IR) injury (12).[3] Conversely, gene transfer–mediated overexpression of BI-1 protects against apoptosis induced by ER stress and IR (10, 11, 13). In this regard, the ER may participate in the initiation of liver regeneration by releasing stored Ca^{2+} (14). Indeed, in many types of cells, including fibroblasts, thymocytes, and epithelial tumor cell lines, intracellular Ca^{2+} is essential for the transition from resting to proliferative state (15). During liver regeneration, several growth factors [epidermal growth factor (EGF), hepatocyte growth factor (HGF), etc.] and hormone receptors (vasopressin and phenylephrine) induce increases in cytosolic intracellular Ca^{2+} via the second messenger

Note: Supplementary data for this article are available at Cancer Research Online (http://cancerres.aacrjournals.org/).

Requests for reprints: John C. Reed, Burnham Institute for Medical Research, 10901 North Torrey Pines Road, La Jolla, CA 92037. Phone: 858-795-5300; Fax: 858-646-3194; E-mail: reedoffice@burnham.org.

doi:10.1158/0008-5472.CAN-06-0850

[3] Unpublished data.

inositol 1,4,5-trisphosphate, which releases stored Ca^{2+} from the ER (14, 16). Interestingly, the BI-1 protein has been shown to regulate Ca^{2+} handling by the ER. Overexpression of BI-1 protein reduces the amounts of Ca^{2+} released in response to drugs that inhibit the ER Ca^{2+}-ATPase (e.g., thapsigargin), whereas BI-1 deficiency increases the efflux of ER Ca^{2+} (12). Thus, it is reasonable to suspect a role for BI-1 in modulating ER handling of Ca^{2+} in hepatocytes.

Interestingly, several Bcl-2 family proteins reside at least in part in ER membranes, where they seem to control levels of releasable Ca^{2+} in this organelle (17–20). Overexpression of antiapoptotic Bcl-2 protein decreases the levels of Ca^{2+} released from the ER in response to thapsigargin (18, 20). In contrast, knocking down Bcl-2 protein expression or overexpressing the proapoptotic Bax protein leads to increases in the amounts of Ca^{2+} released from this organelle after thapsigargin stimulation (17, 21). Moreover, an effect on cell cycle entry by Bcl-2 family proteins has been described (see ref. 22 for review). Bcl-2 overexpression in the liver of transgenic mice delays hepatocyte cell cycle progression during liver regeneration (23). A similar phenotype is also observed in Bcl-2–overexpressing B and T cells (24, 25). Conversely, Bcl-2–deficient T cells showed accelerated cell cycle progression (25). Similarly, in transgenic mice overexpressing Bax in T cells, increased numbers of cycling thymocytes are found and mature T cells enter S phase in response to IL-2 stimulation faster than control cells (26).

These observations with Bcl-2/Bax family proteins therefore prompted us to explore whether *bi-1*–deficient mice display alterations in cell cycle entry and proliferation *in vivo*. Because *bi-1* is prominently expressed in liver (but not thymus or lymphoid tissues; ref. 12), we chose a model of liver regeneration for these studies. Accordingly, we compared *bi-1* (+/+) and *bi-1* (−/−) mice subjected to partial hepatectomy with respect to the kinetics of liver regeneration and molecular events associated with hepatocyte proliferation, such as induction of cyclins, phosphorylation of Rb, and incorporation of bromodeoxyuridine (BrdUrd). The findings suggest an important role for the endogenous *bi-1* gene in regulating liver regeneration and reveal parallels between BI-1 and antiapoptotic members of the Bcl-2 family.

Materials and Methods

Mice. The *bi-1*–deficient mouse line used for these studies has been described previously (12). Mice on a C57BL/6 background at 8 to 10 weeks of age were used for all experiments in this study, comparing $bi\text{-}1^{-/-}$ animals with $bi\text{-}1^{+/+}$ littermates. Mice were housed in a temperature-controlled room with a 12-h dark/12-h light cycle. Food and water were provided *ad libitum*. Mice were maintained in specific pathogen-free housing and cared for accordance with NIH guidelines for animal care.

Partial hepatectomy and tissue sampling. For liver regeneration studies, 8- to 10-week-old $bi\text{-}1^{-/-}$ and $bi\text{-}1^{+/+}$ mice were anesthetized with methoxyflurane and subjected to midventral laparotomy with a two-third liver resection according to the method of Higgins and Anderson (27). The left and right median and left lateral lobes were removed without injuring the remaining liver tissue. Four to six mice from each group were sacrificed before or at different times after hepatectomy. In cases of severe morbidity (lethargy, trembling, anorexia, or body temperature loss), animals were sacrificed and excluded from the analysis. The remnant liver was harvested and the wet weight was measured. A portion of liver was snap frozen in liquid nitrogen for protein and RNA isolation, whereas another portion was embedded in OCT compound for preparation of cryosections (5 μm thick) using a microtome followed by mounting on glass slides. The sectioned tissues were used for microscopy evaluation after staining for analysis of BrdUrd incorporation (see below).

Evaluation of DNA synthesis in hepatocytes. To assess the proliferative response of hepatocytes, DNA synthesis was monitored by BrdUrd (Sigma, St. Louis, MO) incorporation into the nuclei. For pulse-labeling experiments, mice received 50 μg/g (body weight) BrdUrd i.p. injection in 0.2% solution in PBS 2 h before sacrifice. Immunohistochemical staining of BrdUrd was done using Cell Proliferation kit (Amersham Biosciences Corp., Piscataway, NJ) The percentage of BrdUrd-labeled hepatocytes were determined by counting positively stained nuclei in 10 high-power fields (×400 magnification).

Cell isolation, culture, and DNA synthesis measurements. Hepatocytes from mice liver were isolated by collagenase disruption (28) exactly as described before (29). Isolated cells were plated on collagen type I–coated dishes in medium I consisting of Williams' medium E with 10% fetal bovine serum, penicillin (50 IU/mL), streptomycin (50 μg/mL), and insulin (0.1 IU/mL). Hepatocyte viability was at least 90%. Hepatocytes were incubated 4 h at 37°C in a humidified atmosphere with 95% air and 5% CO_2, allowing cell attachment to plates. Medium was then changed and replaced by medium II, which was identical except that it did not contain serum and was supplemented with hydrocortisone hemisuccinate (1 μmol/L) and bovine serum albumin (BSA; 240 μg/mL). Hepatocytes were seeded at 35×10^3 cells per well (96-well plates), cultured for 48 to 96 h in normal medium II (CNTL), or treated with medium containing 25 ng/mL EGF, 20 ng/mL IL-6, 50 ng/mL TNF-α, or combinations of these agents. To measure DNA synthesis, 1.5 μCi (1 Ci = 37 GBq) of [^{3}H]methylthymidine were added per 100 μL of culture and cultures were continued for 12 h.

For terminal deoxynucleotidyl transferase (TdT)–mediated dUTP nick end labeling (TUNEL) assays, hepatocytes were cultured for 24 to 72 h on 13-mm glass coverslips in 24-well plates. Cells were fixed in 4% paraformaldehyde for 30 min on coverslips and then permeabilized using PBS (pH 7.4), 0.1% Triton X-100, and 0.1% sodium citrate for 2 min. After washing, the coverslips were incubated at 37°C for 1 h in a humidified chamber with the TUNEL reaction mixture containing 0.4 IU/μL TdT, 2.5 mmol/L $CoCl_2$, and 2 μmol/L Bodipy FL-14-dUTP, washed in PBS, and mounted in "antifade" medium, and the cells were analyzed under a fluorescence microscope as described previously (29).

For assessment of apoptosis after partial hepatectomy, regenerated liver specimens were frozen in OCT compound and sectioned at 5 μm for processing by the TUNEL method using a commercial kit using 3,3′-diaminobenzidine (DAB) peroxidase substrate (Roche Applied Science, Indianapolis, IN) and counterstained with 0.5% (w/v) methyl green. Specimens were evaluated by UV microscopy at high power magnification (×400) in a blinded fashion. A total of 30 random fields was counted for each TUNEL-stained tissue sample.

Immunoblot analysis. Total liver proteins were isolated from snap-frozen tissues by homogenization in radioimmunoprecipitation assay buffer [50 mmol/L Tris-HCl (pH 7.4), 150 mmol/L NaCl, 1% Triton X-100, 1% sodium deoxycholate, 2 mmol/L phenylmethylsulfonyl fluoride, 1 mmol/L EDTA, 10 μg/mL leupeptin, 10 μg/mL aprotinin] supplemented with 0.2% SDS. Protein concentration was estimated by the bicinchoninic acid protein assay kit using BSA as the standard. Total protein (50 μg) aliquots were loaded onto either 8%, 10%, or 12.5% SDS-polyacrylamide gels and electrophoretically transferred onto nitrocellulose membranes. After blocking with 6% nonfat skim milk in TTBS [10 mmol/L Tris-HCl (pH 7.5), 140 mmol/L NaCl, 0.05% Tween 20] for 1 h at 37°C, membranes were incubated with primary antibody in TS-TMBSA [Tris/sodium chloride buffer (pH 7.6–7.8) with 0.1% Tween 20, 5% skim milk, and 2% BSA (pH 7.4–7.6)], washed with TTBS, and incubated for 1 h at room temperature with horseradish peroxidase–conjugated secondary antibodies anti-mouse immunoglobulin G or anti-rabbit immunoglobulin G (Amersham Biosciences). After washing with TTBS, blots were developed using an enhanced chemiluminescence (ECL) detection kit (Amersham Biosciences) and BioMax ML film (Eastman Kodak, Rochester, NY). The blot was reprobed with the following antibodies: rabbit polyclonal anti–cyclin D1 antibody (1:1,000 dilution; Santa Cruz Biotechnology, Santa Cruz, CA), mouse monoclonal anti–cyclin D3 antibody (1:2,000 dilution; Transduction Laboratories BD, San Diego, CA), mouse monoclonal anti–cyclin B antibody (1:2,500 dilution; Transduction Laboratories), rabbit polyclonal anti–cyclin A antibody (1:2,000 dilution; Santa Cruz Biotechnology), rabbit polyclonal anti–cyclin E antibody (1:500 dilution; Santa Cruz

Biotechnology), mouse monoclonal anti-Cdk2 antibody (1:2,500 dilution; Transduction Laboratories), mouse monoclonal anti-Cdk4 antibody (1:2,500 dilution; Transduction Laboratories), human monoclonal anti-Rb (1:1,000 dilution; Transduction Laboratories), human monoclonal anti-p21 (1:500 dilution; Transduction Laboratories), human monoclonal anti-p27 (1:1,000 dilution; Transduction Laboratories), and anti-tubulin antibody (1:500 dilution; Santa Cruz Biotechnology).

RNA extraction and reverse transcription quantitative PCR. Total RNA was extracted from mouse liver by an acid guanidium thiocyanate-phenol-chloroform extraction method with RNA STAT-60 (Tel-Test "B," Inc., Friendswood, TX). RNA was reverse transcribed by Moloney murine leukemia virus reverse transcriptase (Invitrogen, San Diego, CA) using random hexamers (Life Technologies). Specific primers for murine genes included the following: TNF-α, 5′-ACAGAAAGCATGATCCGCG-3′ (forward) and 5′-GCCCCCCATCTTTTGGG-3′ (reverse); IL-6, 5′-CTGCAAGAGACTTCCATCCAGTT-3′ (forward) and 5′-GAAGTAGGGAAGGCCGTGG-3′ (reverse); HGF, 5′-ATCATTGGTAAAGGAGGCAGCTAT-3′ (forward) and 5′-AATTCCAAGGCTGGCATTTG-3′ (reverse); c-Fos, 5′-CGGGTTTCAACGCCGAC-3′ (forward) and 5′-TGGCACTAGAGACGGACAGATC-3′ (reverse); c-Jun, 5′-CGATGCCCTCAACGCC-3′ (forward) and 5′-CTTAGGGTTACTGTAGCCGTAGGC-3′ (reverse); BI-1, 5′-TGGCTGATGGCAACACCTC-3′ (forward) and 5′-GGCGAAGCCAGCGAGA-3′ (reverse); STAT3, 5′-CACCAACGACCTGCAGCA-3′ (forward) and 5′-TGCATCAATGAATCTAAAGTGCG-3′ (reverse); Rel-A, 5′-CATCGAACAGCCGAAGCAA-3′ (forward) and 5′-TGCCCGCTGAGCGC-3′ (reverse); Rel-B, 5′-GTGCCGACTTCTCTCAAGCTG-3′ (forward) and 5′-GGGTGGCGTTTTGAACACA-3′ (reverse); and c-Myc, 5′-ATGTTGCGGTCGCTACGTC-3′ (forward) and 5′-AGAAGTTGCCACCGCCG-3′ (reverse).

Real-time PCR was done with iTaq polymerase in a Bio-Rad iCycler (Hercules, CA) using iTaq together with SYBR Green detection according to the manufacturer's protocol, with 12 ng of total cDNA, 50 nmol/L of each primer, and 1× iTaq SYBR Green Supermix in a total volume of 25 μL.

Cytokine assays. The BD Cytometric Bead Array (CBA) Mouse Inflammation kit was used to quantitatively measure TNF-α and IL-6 by flow cytometry.

Statistics. For most experiments, data were expressed as mean ± SD. Statistical significance of differences between various samples was determined by *t* test or Mann-Whitney *U* test.

Results

***Bi-1* deficiency increases proliferation *in vitro* of hepatocytes.** Although *bi-1* is ubiquitously expressed at the mRNA level in mammalian tissues, the highest levels of *bi-1* mRNA are found in liver, kidney, and testes. We therefore tested effects of *bi-1* deficiency on replication of hepatocytes in primary culture. Quiescent hepatocytes isolated from adult liver can be stimulated to proliferate in culture with various cytokines and growth factors. We therefore measured DNA replication (as determined by [^{3}H]thymidine incorporation) in cultured hepatocytes isolated from *bi-1* KO mice and wild-type (WT) littermates after stimulation with TNF-α, EGF, IL-6, or combinations of these agents. When stimulated with the combination of EGF and TNF-α, [^{3}H]thymidine incorporation was approximately double in BI-1–deficient hepatocytes compared with WT cells when measured at 72 to 96 h after plating (Fig. 1*A*; data not shown). Measurements of DNA synthesis at earlier times (48 h) produced similar results (Supplementary Fig. S1), suggesting that loss of normal differentiation cannot account for differences in *bi-1*$^{+/+}$ versus *bi-1*$^{-/-}$ hepatocytes. The incorporation of [^{3}H]thymidine by BI-1–deficient hepatocytes also tended to be higher when stimulated individually with cytokines or growth factors but did not reach statistical significance (Fig. 1*A*). Thus, at least when supplied with certain combinations of known hepatocyte mitogens, BI-1–deficient cells exhibit increased DNA synthesis responses compared with BI-1–expressing hepatocytes. No difference in cell viability or apoptosis was detected by trypan blue dye exclusion (data not shown) or TUNEL assay (Supplementary Fig. S2), respectively, in cultures of *bi-1*$^{-/-}$ and *bi-1*$^{+/+}$ hepatocytes.

Accelerated onset of DNA synthesis and mitosis *in vivo* in *bi-1*–deficient liver. To examine the effects of BI-1 deficiency on the restoration of the liver mass after partial hepatectomy, we compared the wet weight of livers of *bi-1*$^{+/+}$ and *bi-1*$^{-/-}$ animals at various times after surgical removal of two thirds of their livers. The remnant liver weight was compared relative to body weight for all measurements. As shown in Fig. 1*B*, liver weight restoration occurred with accelerated kinetics in *bi-1*$^{-/-}$ compared with *bi-1*$^{+/+}$ mice. However, the absolute increase in liver weight was similar for the two groups of mice, with liver weights returning to preoperative levels at 36 h for *bi-1*$^{-/-}$ mice compared with 48 h for *bi-1*$^{+/+}$ animals.

Next, studies were done to compare the proportion of cycling hepatocytes in *bi-1*$^{-/-}$ and *bi-1*$^{+/+}$ mice based on *in vivo* incorporation of BrdUrd into DNA (7, 8). Consistent with previous reports (7, 8, 30), evidence of increased incorporation of BrdUrd into regenerating liver of WT mice was first detectable at 36 h after partial hepatectomy (Supplementary Fig. S3). In these normal *bi-1*$^{+/+}$ mice, hepatocyte replication reached maximum by 40 h and then began to diminish by 48 h after surgery (Fig. 1*C*). In contrast, hepatocyte DNA replication in regenerating *bi-1*$^{-/-}$ mice was significantly elevated by 32 h after partial hepatectomy (Fig. 1*C*; Supplementary Fig. S1). Similar to normal mice, the percentage of cycling cells reached maximum at 40 h after partial hepatectomy and began to decline thereafter. However, the rate of decline in actively cycling hepatocytes was faster in *bi-1*$^{-/-}$ mice, with very few hepatocytes incorporating BrdUrd at 68 h after partial hepatectomy. Thus, DNA replication begins sooner and ends sooner in *bi-1*$^{-/-}$ livers.

Consistent with the BrdUrd incorporation results, analysis of the percentage of mitotic cells in livers resected from *bi-1*$^{-/-}$ and *bi-1*$^{+/+}$ mice at various times after partial hepatectomy showed a more rapid rise in the prevalence of mitotic cells and more rapid return toward normal in BI-1–deficient mice (Fig. 1*D*). The time at which peak mitotic cell (M phase) accumulation occurred in WT mice was later than peak BrdUrd labeling (S phase) as expected. In contrast, the percentages of apoptotic cells in livers of *bi-1*$^{+/+}$ and *bi-1*$^{-/-}$ mice (as measured by TUNEL assay) were not significantly different at 48 to 168 h after partial hepatectomy (Supplementary Fig. S3), suggesting that differences in apoptosis do not contribute to the more rapid kinetics of liver growth in BI-1–deficient mice.

Accelerated expression of cyclins in regenerating *bi-1*–deficient mice. Because DNA replication was accelerated in the regenerating livers of BI-1 KO mice, we compared the kinetics of cyclin proteins expression in *bi-1*$^{-/-}$ and *bi-1*$^{+/+}$ mice. For these experiments, lysates were prepared from liver tissue resected from partial hepatectomy–treated animals, normalized for total protein content, and analyzed by immunoblotting using antibodies recognizing various cyclin family proteins. In agreement with the accelerated DNA replication and mitosis observed in regenerating *bi-1*$^{-/-}$ hepatocytes, increases in cyclin D1 were detected earlier in *bi-1*$^{-/-}$ mice (Fig. 2*A*). Cyclin D1 protein levels were also higher in regenerating liver tissue recovered from *bi-1*$^{-/-}$ mice at several times analyzed after partial hepatectomy compared with *bi-1*$^{+/+}$ mice. The rise, subsequent decline, and rise again in cyclin D1 protein levels probably reflect synchronized cycles of hepatocyte cell replication in these regenerating livers, producing a biphasic pattern of cyclin D1 expression in which the second peak coincides

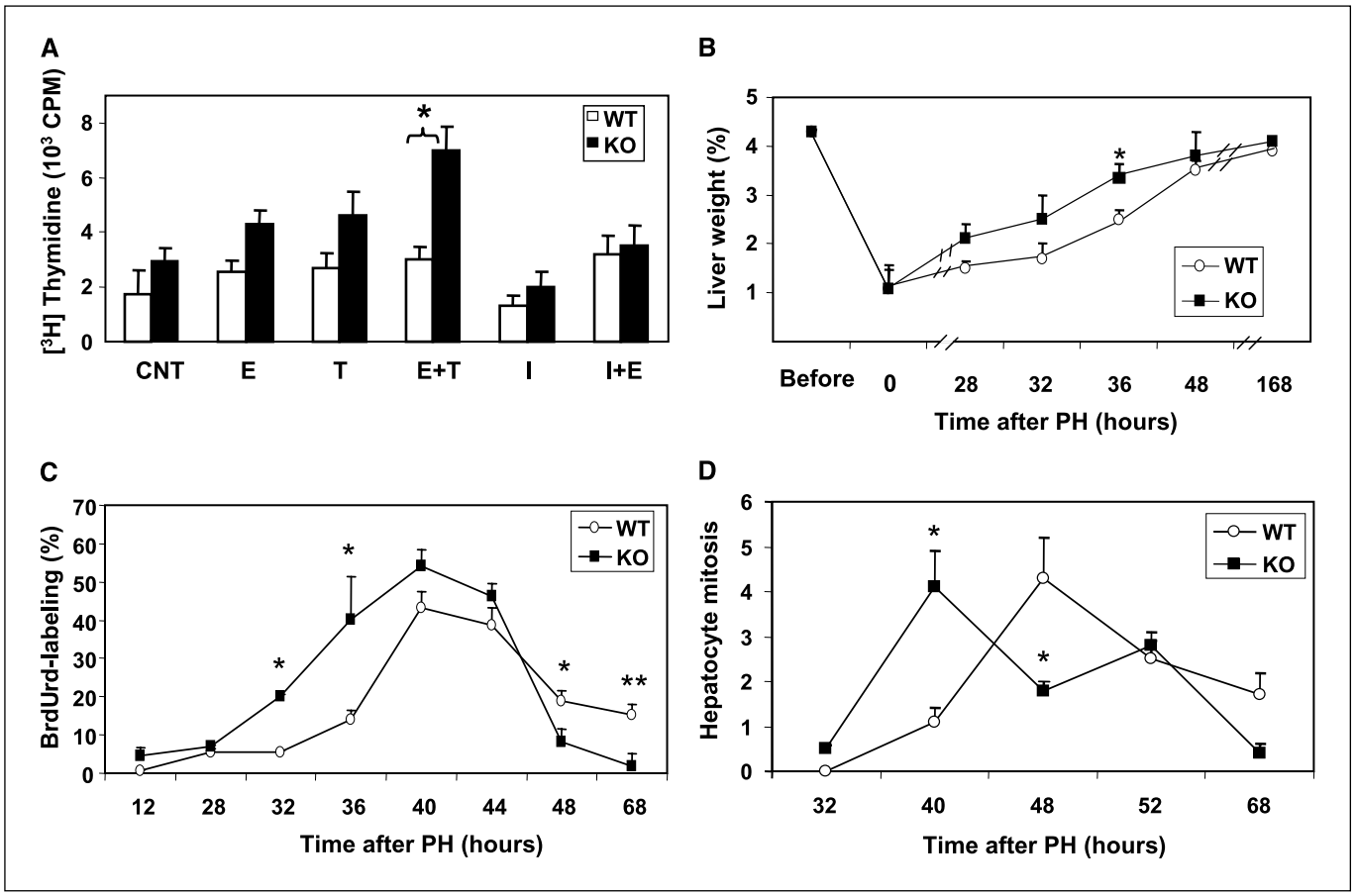

Figure 1. Accelerated liver regeneration in *bi-1*$^{-/-}$ mice. *A,* hepatocytes from *bi-1*$^{-/-}$ (*KO*) and *bi-1*$^{+/+}$ (*WT*) mice were cultured for 72 and 96 h in control medium (*CNT*) or in medium containing 25 ng/mL EGF (*E*), 20 ng/mL TNF (*T*), 50 ng/mL IL-6 (*I*), or combinations of these agents. Cells were pulsed with 1.5 μCi of [^{3}H]methylthymidine for 12 h before collecting DNA. *Columns,* mean (n = 3) [^{3}H]methylthymidine incorporation (cpm) from three mice of each genotype; *bars,* SD. *B,* recovery of liver weight after partial hepatectomy (*PH*). The results are expressed as a percentage of liver weight relative to body weight. *Points,* mean of four to six mice per group at each time point; *bars,* SD. *C,* percentage of S-phase hepatocytes were determined by pulse labeling with BrdUrd for 2 h. The *bi-1*$^{+/+}$ and *bi-1*$^{-/-}$ mice were subjected to partial hepatectomy and injected with BrdUrd 2 h before sacrifice. The remnant liver was fixed, sectioned, and stained with an anti-BrdUrd antibody. Nuclei were counterstained with 4′,6-diamidino-2-phenylindole. Data represent percentage of BrdUrd-positive cells based on counting at least 3,000 total nuclei. *Points,* mean based on three to six regenerating livers; *bars,* SD. *D,* kinetics of hepatocyte mitosis after partial hepatectomy. Mitotic figures were counted in liver tissue at the indicated times after partial hepatectomy. Data represent percentage of mitosis relative to hepatocytes based on three regenerating livers. *Points,* mean; *bars,* SD. *, $P < 0.05$; **, $P < 0.001$.

with maximal DNA synthesis at 36 h after partial hepatectomy. Similar results were obtained for cyclin D3, the Cdc2-related protein kinase, and Cdk4 (Fig. 2*B* and *C*). Cdk2 protein levels were low in regenerating liver of both *bi-1*$^{-/-}$ and *bi-1*$^{+/+}$ until 32 h when rises were detected in both groups of animals. However, levels of Cdk2 protein were higher in *bi-1*$^{-/-}$ mice at 32 h and remained persistently elevated compared with *bi-1*$^{+/+}$ animals (Fig. 2*C*). Probing blots with anti-tubulin antibody confirmed loading of equivalent amounts of total protein for all samples.

Accelerated hyperphosphorylation of Rb and degradation of p27^{Kip1} in regenerating liver of *bi-1*–deficient mice. Cyclin/Cdk complexes phosphorylate Rb, causing Rb to release E2F family transcription factors required for transition into S phase (23, 31). For this reason, we analyzed the phosphorylation status of Rb in regenerating livers of *bi-1*$^{-/-}$ and *bi-1*$^{+/+}$ at various times after partial hepatectomy by immunoblotting using a phosphorylated-specific antibody. As shown in Fig. 3*A*, Rb hyperphosphorylation was detectable at 12 h after partial hepatectomy in regenerating *bi-1*$^{-/-}$ liver, peaking at 24 to 28 h, and then declining. In contrast, increases in Rb hyperphosphorylation were not detected until 24 h in regenerating *bi-1*$^{+/+}$ livers, peaking at 44 h after partial hepatectomy. Reprobing blots with a phosphorylated-independent antibody confirmed equivalent amounts of Rb protein in all samples, verifying loading of comparable amounts of protein for all samples. Thus, Rb hyperphosphorylation occurs with accelerated kinetics in BI-1–deficient regenerating liver.

Degradation of the Cdk inhibitors p21 and p27 permits Rb phosphorylation and represents an important event for S-phase entry (32). We therefore examined the levels of p21 and p27 by immunoblotting in regenerating livers of *bi-1*$^{-/-}$ and *bi-1*$^{+/+}$ mice at various times after partial hepatectomy (Fig. 3*B*). Although no difference was observed in p21 expression, p27 protein degradation occurred with accelerated kinetics in BI-1–deficient regenerating liver. As shown in Fig. 3*B*, p27^{Kip} was depleted from liver tissue within 1 h in *bi-1*$^{-/-}$ mice compared with 4 h in *bi-1*$^{+/+}$ animals. Taken together, these findings correlate with the data obtained for expression of cyclins and Cdk family proteins (Fig. 2), showing that BI-1 deficiency accelerates hepatocyte entry into cell cycle following partial hepatectomy.

Increased intrahepatic cytokine gene expression in regenerating livers of *bi-1*–deficient mice. The cytokines TNF-α and IL-6 are among the earliest priming factors that have been

implicated in liver regeneration after loss of parenchymal liver mass (7, 8). We therefore measured TNF-α and IL-6 protein levels in serum after partial hepatectomy (6). At 3 and 6 h after partial hepatectomy, BI-1–deficient mice contained higher serum levels of both TNF-α (2-fold more; Fig. 4*A*) and IL-6 (3.5-fold more; Fig. 4*C*) relative to WT mice as determined by using a CBA method. In contrast, serum levels of IFN-γ were largely unchanged (Fig. 4*C*), thus confirming the specificity of these results.

Next, hepatic expression of these cytokines was investigated at the mRNA level using real-time PCR. The mRNA levels of TNF-α (Fig. 4*B*) and IL-6 (Fig. 4*D*) were significantly higher in the *bi-1*–deficient mice in comparison with WT animals. In contrast, HGF (Fig. 4*D*) mRNA levels were not significantly different (by either Mann-Whitney *U* test or unpaired *t* test), thus serving as a specificity control.

Finally, we also compared the relative levels of mRNA expression of immediate early genes known to be induced in response to TNF-α or IL-6 cytokines (i.e., the NF-κB family members Rel-A, Rel-B, p105, and p100 and the proto-oncogenes c-Fos, c-Jun, and c-Myc). Greater induction of mRNAs encoding c-Fos and Rel-B was observed in *bi-1*$^{-/-}$ compared with *bi-1*$^{+/+}$ mice at 1 h after partial hepatectomy (Fig. 5*A* and *B*). In contrast, STAT3, Rel-A, c-Jun, and p100 mRNA levels did not differ (Fig. 5; data not shown), thus serving as a specificity control. We also found that E2F2 mRNA levels were higher at 1 h after partial hepatectomy in *bi-1*$^{-/-}$ compared with *bi-1*$^{+/+}$ mice, consistent with the more rapid kinetics of cell cycle entry found for BI-1–deficient hepatocytes and correlating with the data obtained for Rb phosphorylation. In contrast, levels of E2F1 and E2F3 were not different in *bi-1*$^{+/+}$ versus *bi-1*$^{-/-}$ liver partial hepatectomy (Fig. 5; data not shown). In WT mice, levels of endogenous *bi-1* mRNA declined in liver after partial hepatectomy (Fig. 5*C*), indicating that reductions in *bi-1* expression are associated with entry to cell cycle in hepatocytes *in vivo*. In contrast, levels of Mcl-1 mRNA did not change significantly, thus serving as a specificity control (Fig. 5*C*).

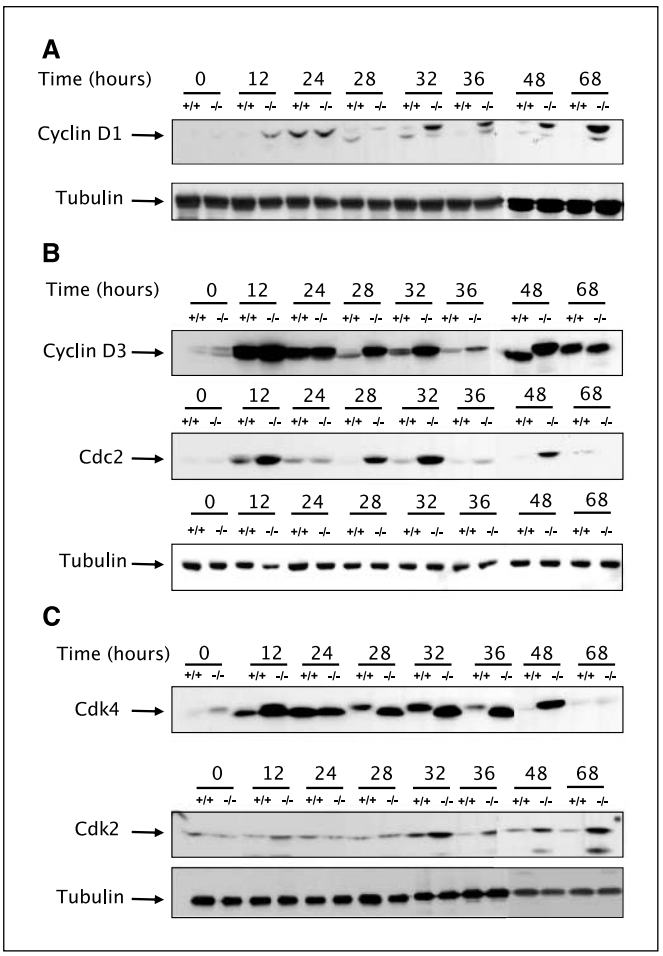

Figure 2. Accelerated expression of cyclin family proteins in regenerating *bi-1*–deficient livers. Livers were harvested at various times from 0 to 68 h after partial hepatectomy. Equal amounts of total extracts were loaded onto 12% SDS-polyacrylamide gels and transferred to nitrocellulose membranes. Blots were incubated with anti–cyclin D1 (*A*), anti-Cdc2 (*B*), or anti-Cdk2 and anti-Cdk4 (*C*) antibodies followed by detection using an ECL method. Three mice per time point were examined. All blots were reprobed with anti-tubulin antibody as a control for loading and membrane transfer.

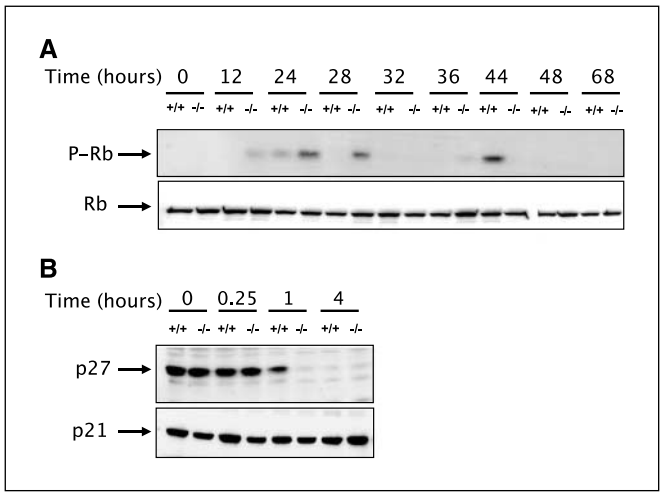

Figure 3. Disruption of BI-1 accelerates Rb hyperphosphorylation and p27^{Kip} degradation in regenerating livers. Livers were harvested at 0 to 68 h after partial hepatectomy. Equal amounts of total extracts were loaded into 8% SDS-polyacrylamide gels for Rb detection and into 12% SDS-polyacrylamide gels for p21 and p27 analysis. Proteins were transferred to nitrocellulose membranes, which were incubated with antibodies specific for Rb or phosphorylated Rb (*P-Rb*; *A*) or p21 or p27 (*B*). Data are representative of three independent experiments.

Dephosphorylation of nuclear factor of activated T cells 1 is accelerated in BI-1–deficient livers after partial hepatectomy. Elevations in intracellular Ca^{2+} concentrations occur during cell cycle entry in hepatocytes during liver regeneration (33–35). Of relevance to cell proliferation, this increase in intracellular Ca^{2+} has been correlated with activation of the calmodulin-dependent phosphatase calcineurin (36, 37). Calcineurin dephosphorylates and promotes the nuclear translocation of nuclear factor of activated T cells (NFAT), which regulates the induction of multiple genes, including *TNF-α* (37). Although NFAT1 is widely expressed among tissues (37), no studies have thus far addressed the function of NFAT1 during liver regeneration.

Because BI-1 has been shown to regulate Ca^{2+} handling by the ER (12), we hypothesized that absence of this protein would coincide with an alteration in calcineurin-dependent dephosphorylation of NFAT. Accordingly, we used phosphorylated-specific antibodies to assess the phosphorylation status of NFAT1 by immunoblotting in regenerating livers from *bi-1*$^{-/-}$ and *bi-1*$^{+/+}$ mice. In *bi-1*$^{-/-}$ mice, levels of phosphorylated NFAT1 declined rapidly in lysates prepared from regenerating liver, consistent with Ca^{2+}/calcineurin-dependent dephosphorylation (Fig. 6*A*). In contrast,

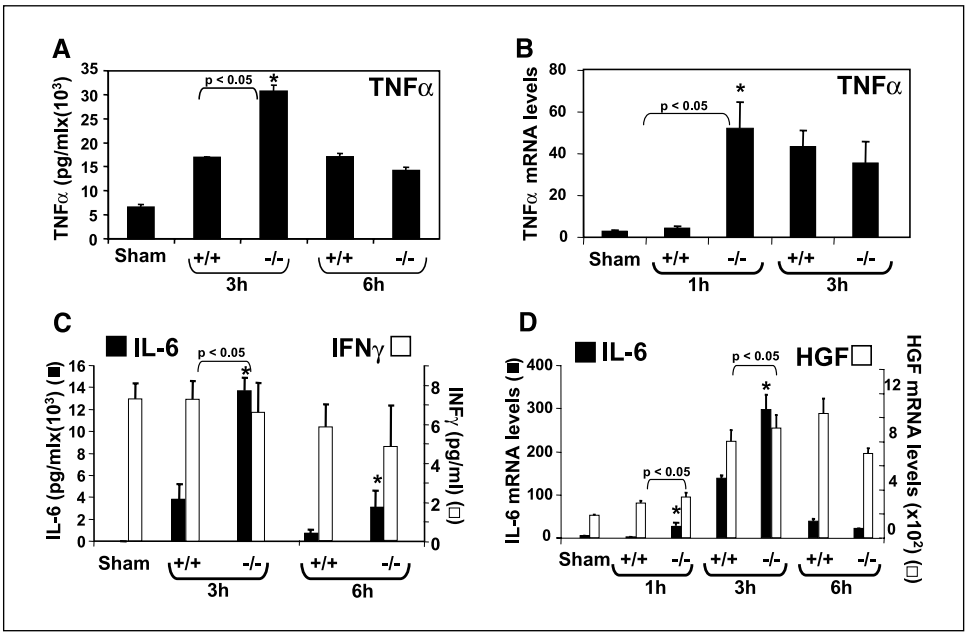

Figure 4. Increased elaboration of TNF-α and IL-6 cytokines in *bi-1*–deficient mice after partial hepatectomy. Serum levels of TNF-α, IL-6, and IFN-γ (*A* and *C*) proteins and liver levels of TNF-α, IL-6, and IFN-γ (*B* and *D*) mRNA levels were measured before and at various times after partial hepatectomy. Protein levels were assessed by a fluorescence-activated cell sorting–based method, whereas RNA levels were evaluated by real-time reverse transcription-PCR, normalizing RNA relative to 18S rRNA. Similar results were obtained by normalizing with L32 or cyclophilin mRNAs (data not shown). *Columns,* mean of three mice for each condition shown; *bars,* SD. *, $P < 0.05$.

NFAT1 dephosphorylation was slower and less extensive in regenerating *bi-1*$^{+/+}$ liver. Probing blots with a phosphorylated-independent NFAT antibody confirmed loading of equivalent amounts of protein for all samples.

Next, we analyzed NFAT1 localization by immunohistochemistry, comparing the percentages of hepatocytes with nuclear versus cytosolic NFAT1 in tissue sections from regenerating livers of *bi-1*$^{-/-}$ and *bi-1*$^{+/+}$ mice (Fig. 6*B* and *C*). At 15 min after partial hepatectomy in *bi-1*$^{-/-}$ mice, NFAT1 staining was found in the nuclei of most hepatocytes and was essentially absent from the cytosol. In contrast, NFAT1 staining remained predominantly in the cytosol of *bi-1*$^{+/+}$ hepatocytes at 15 min after partial hepatectomy, with few cells exhibiting nuclear staining. We conclude therefore that BI-1 deficiency markedly alters activation-induced nuclear translocation of NFAT1 in the setting of liver regeneration.

Discussion

We report here that the ER protein BI-1 regulates hepatocyte proliferation *in vivo* following partial hepatectomy. We showed that BI-1 deficiency accelerates liver regeneration after partial hepatectomy. Regenerating hepatocytes of BI-1–deficient mice enter cell cycle faster as documented by more rapid accumulation of BrdUrd-incorporating cells, associated with earlier increases in cyclin D1, cyclin D3, Cdk2, and Cdk4 protein levels, more rapid hyperphosphorylation of Rb, and faster degradation of p27. BI-1 deficiency, however, does not disturb the homeostatic mechanisms responsible for cessation of hepatocyte proliferation once liver size has been restored, as liver weights of *bi-1*$^{-/-}$ mice did not exceed normal values after completion of regeneration.

The mechanisms by which BI-1 regulates hepatocyte emergence from quiescence and entry into cell cycle remain to be delineated. We hypothesize, however, that the ability of BI-1 to regulate Ca^{2+} accumulation by the ER may play a role. In this regard, we recently observed a role for the BI-1 protein in suppressing cell death linked to ER stress in cultured primary hepatocytes and other types of cells (12). Among the inducers of ER stress to which BI-1 deficiency increased sensitivity is thapsigargin, a selective inhibitor of the Ca^{2+}-ATPase of the ER that induces cell death due to a leakage of Ca^{2+} from the ER into the cytosol. Ca^{2+} imaging studies showed that loss of BI-1 results in an increase in the pool of thapsigargin-releasable intracellular Ca^{2+}, whereas BI-1 overexpression reduces the amount of intracellular Ca^{2+} released from ER by thapsigargin treatment (12). Thus, because ER Ca^{2+} plays important roles in G_0-G_1 transition and progression to S phase (16, 22), it is conceivable that the effects of BI-1 on ER Ca^{2+} homeostasis directly or indirectly account for the accelerated proliferation of hepatocytes seen in this model of liver regeneration. Consistent with this hypothesis, we observed in regenerating *bi-1*$^{-/-}$ liver more rapid dephosphorylation and nuclear translocation of NFAT1, a Ca^{2+}-dependent event linked to calcineurin activation.

Although BI-1 deficiency perturbed NFAT1 regulation in regenerating liver, a causal role for accelerated NFAT1 activation in more rapid hepatocyte cell cycle entry *in vivo* cannot be inferred from these data alone. Many diverse cellular functions are regulated by alterations in intracellular Ca^{2+}, including secretion, cytoskeleton organization, protein synthesis and folding, and gene expression, in addition to cell cycle entry and progression. Thus, multiple cellular pathways could be altered by effects of BI-1 on ER Ca^{2+} homeostasis. Nevertheless, given the role of cytokines in "priming" hepatocytes for cell division and the recognized role of NFAT family transcription factors in controlling cytokine gene expression (22, 24), it might be speculated that increased accumulation of Ca^{2+} in BI-1–deficient cells results in enhanced or accelerated activation of the calcineurin-NFAT axis, thereby promoting cytokine gene expression and facilitating hepatocyte entry into cell cycle (as manifested by earlier increases in cyclin D1, cyclin D3, Cdk2, and Cdk4 protein levels and by more rapid hyperphosphorylation of Rb). However, because BI-1 deficiency also resulted in increased proliferation *in vitro* of isolated hepatocytes treated with exogenous growth factors and cytokines, a cell autonomous role of BI-1 in controlling cell cycle entry and/or S-phase progression also seems likely.

The observation that regenerating liver in *bi-1*$^{-/-}$ mice has more *c-fos* expression could be a manifestation of the increased production of IL-6 or TNF-α, both of which are known to induce

c-fos expression (38, 39). Conversely, c-Fos protein is reported to enhance *IL-6* gene promoter activity in collaboration with STAT3 in HepG2 hepatocellular carcinoma cells (40), raising the possibility that c-Fos accounts for elevated IL-6 production in *bi-1*$^{-/-}$ mice.

Our findings for BI-1 are similar to results obtained previously during studies of Bcl-2 family proteins with respect to their effects on cell proliferation, thus implying commonalities in the cellular mechanisms regulated by these two classes of proteins. For example, studies of transgenic mice overexpressing antiapoptotic protein Bcl-2 in liver showed that Bcl-2 expression delays hepatocyte cell cycle progression during liver regeneration by delaying the increase of proliferating cell nuclear antigen, cyclin E, cyclin E–associated kinase activity, cyclin A, and p107 (41). A similar phenotype was observed in T cells overexpressing Bcl-2, which led to sustained levels of Cdk inhibitor p27, correlating with prolonged G_1 phase (24). Consistent with a role in controlling cell proliferation, other studies have also found effects of Bcl-2 overexpression on the Rb/E2F complex and on p21 expression (42). Conversely, Bcl-2–deficient T cells showed increased cell cycle progression and acceleration degradation of p27 (25). The accelerated cell cycle progression in Bcl-2–deficient T cells involved nuclear translocation of NFAT (24). In contrast to antiapoptotic protein Bcl-2, it has also been shown, using transgenic mice, that overexpressing proapoptotic protein Bax in T cells increased the number of cycling thymocytes and that mature T cells enter S phase in response to IL-2 stimulation faster than control cells (26). This effect of Bax was associated with an earlier decline in $p27^{Kip1}$ levels.

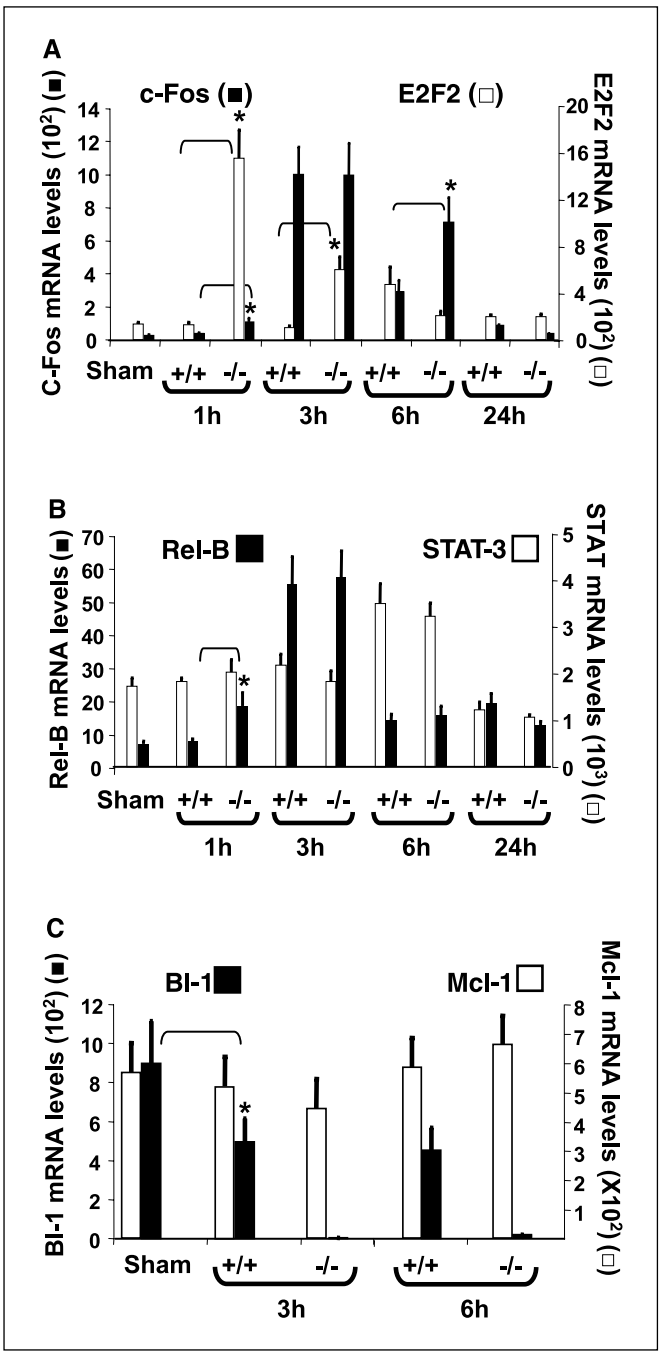

Figure 5. Comparison of induction of immediate early genes in *bi-1*$^{-/-}$ and *bi-1*$^{+/+}$ mice following partial hepatectomy. Quantitative PCR was used to compare mRNA levels for c-Fos, Rel-B, E2F2, STAT3, BI-1, and Mcl-1. Total RNA was isolated from liver at time 0 (*Sham*) and at various times after partial hepatectomy. Results were normalized relative to 18S rRNA. Similar results were also obtained by normalization using L32 or cyclophilin mRNA (data not shown). *Columns,* mean (arbitrary units) based on analysis of three animals for each condition and analyzing specimens from each animal in triplicate; *bars,* SD. *, $P < 0.05$.

Bcl-2 and Bax also have in common with BI-1 that they regulate Ca^{2+} handling by the ER (reviewed in refs. 43, 44). Overexpression of Bcl-2 phenocopies the effects on ER Ca^{2+} produced by BI-1 overexpression, with both proteins reducing the pool of thapsigargin-releasable Ca^{2+} (17, 18, 20). Studies using ER-targeted, Ca^{2+}-sensitive fluorescent proteins have provided evidence that Bcl-2 overexpression reduces the basal concentration of free Ca^{2+} in the lumen of the ER (17), and we have obtained similar results for BI-1–overexpressing cells using this technology.[3] Ablation of the genes encoding proapoptotic proteins Bax and Bak also produces a similar ER phenotype as overexpression of BI-1 with respect to Ca^{2+} regulation (17, 21). Altogether, therefore, this study of the effects of BI-1 deficiency on liver regeneration reveals additional similarities between BI-1 and Bcl-2/Bax family proteins, showing a role for BI-1 in regulating cell proliferation *in vivo*, in addition to its previously described actions as a regulator of apoptosis.

More rapid induction of genes encoding transcription factors, c-Fos, c-Myc, and Rel-B was observed in *bi-1*$^{-/-}$ liver. Many cytokine receptors trigger rapid expression on these genes, which may account for the biphasic expression of c-Fos observed in time course studies of the partial hepatectomy model. Thus, expression of c-Fos, c-Myc, and Rel-B is presumably induced by the surgical liver resection, with ensuing cytokine production inducing a second wave of signals that triggers or maintains c-Fos, c-Jun, and c-Myc expression. In this regard, the promoters of the *TNF-α* and *IL-6* genes have been reported to directly bind and to be transactivated by c-Fos and c-Jun (45, 46).

It is well know that a potential connection exists between Bcl-2 and liver tumorigenesis. Bcl-2 overexpression delays the development and reduces the frequency of transforming growth factor-α (TGF-α)–induced liver tumors in transgenic mice (41). Studies also showed that Bcl-2 expression inhibits liver tumor development in *c-myc* transgenic mice (47) as well as in mice injected with the carcinogen diethylnitrosamine (5, 23). Data support the hypothesis that the delay in hepatocarcinogenesis in Bcl-2 transgenic mice is predominantly due to a direct effect of Bcl-2 on hepatocyte cell cycle progression (23). Our results presented in this study and the previous results showing *in vitro* binding of BI-1 with Bcl-2 (and Bcl-X_L; ref. 10) suggest that down-regulation of BI-1 protein in liver cancer cells (and other cancers) could accelerate

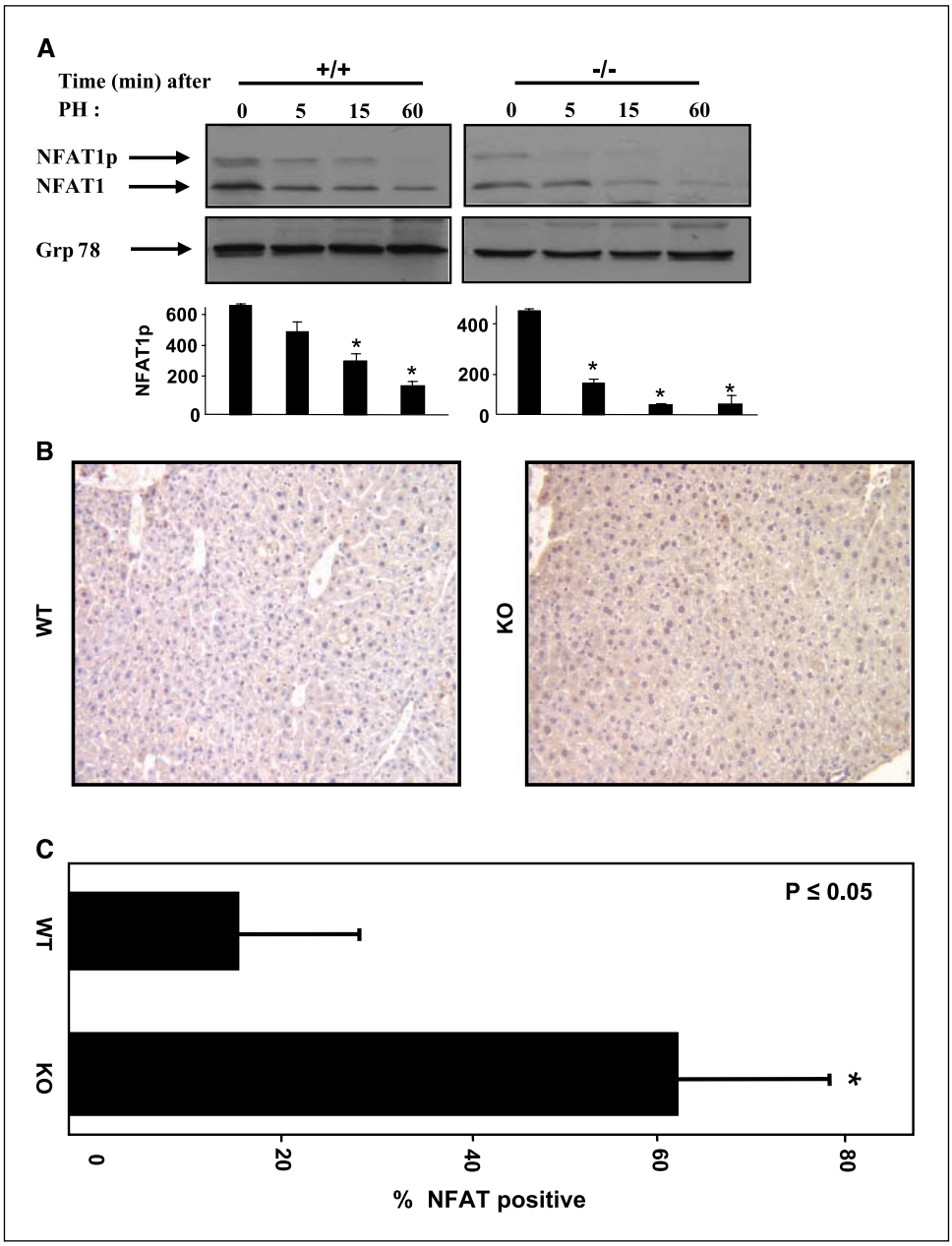

Figure 6. NFAT1 dephosphorylation and nuclear translocation are accelerated in *bi-1*–deficient mouse liver after partial hepatectomy. *A,* livers were harvested at 0 to 5 to 15 min and 1 h after partial hepatectomy. Whole extracts were analyzed by immunoblotting using antibodies specific for NFAT1 and Grp78. *Arrow,* phosphorylated form of NFAT1 (*NFAT1p*). Data were quantified by scanning densitometry, *bottom. Columns,* mean (n = 3–4); *bars,* SE. Statistical significance was determined by t test. *, $P \leq 0.05$. *B* and *C,* BI-1 expression impairs NFAT1 nuclear translocation. Liver sections from *bi-1*$^{+/+}$ (*WT*) and *bi-1*$^{-/-}$ (*KO*) mice were stained with anti-NFAT1 antibody. Antibody detection was accomplished by a colorimetric DAB method (*brown*), and nuclei were counterstained with hematoxylin (*blue*). *B,* representative high-power views. *C,* quantification of data, representing the percentage of NFAT1-positive nuclei based on counting at least 1,500 nuclei. *Columns,* mean (n = 3); *bars,* SD.

hepatocarcinogenesis by removing a restraining influence on cell proliferation. Conversely, up-regulated BI-1 expression in liver conceivably could promote carcinogenesis by inhibiting apoptosis.

A potential connection has been identified between Bcl-2 and liver tumorigenesis. Bcl-2 overexpression delays the development and reduces the frequency of TGF-α–induced liver tumors in transgenic mice (41). Bcl-2 expression inhibits liver tumor development in *c-myc* transgenic mice (48) as well as in mice injected with the carcinogen diethylnitrosamine (41). It has been proposed that the delay in hepatocarcinogenesis in Bcl-2 transgenic mice is predominantly due to a direct effect of Bcl-2 on hepatocyte cell cycle entry or progression (41). Our results presented in this study, when taken together with previous studies showing binding of BI-1 to Bcl-2 (and Bcl-X_L; ref. 10), suggest that BI-1 protein operates in the same pathway as Bcl-2 and Bcl-X_L to suppress cell proliferation. Consequently, *bi-1* overexpression would be expected to delay whereas loss of *bi-1* might be expected to accelerate hepatocellular carcinogenesis because of the effect of BI-1 protein on cell proliferation. On the other hand, the ability of BI-1 to suppress cell death could favor tumorigenesis. In this regard, little is known about the expression of BI-1 in human cancers. Previous studies have shown BI-1 overexpression in prostate carcinoma and prostate cancer cell lines. Moreover, application of RNA interference to reduce BI-1 increases apoptosis of prostate cancer cells, indicating that BI-1 contributes to maintaining the survival of these malignant cells in culture (13). Higher levels of BI-1 mRNA have been described as a prognostic factor in lung adenocarcinoma (49), and tumor-associated increases in BI-1 mRNA expression have also been reported in breast, uterine, and ovarian cancers (49, 50).

Although much remains to be learned about the molecular mechanisms involved, elucidation of the signaling pathways

modulated by BI-1 may provide new insights for improved understanding and possibly treatment of hepatocellular carcinoma and other forms of cancers in the future.

Acknowledgments

Received 3/7/2006; revised 10/23/2006; accepted 12/12/2006.

Grant support: California Breast Cancer Research Program, Fondation pour La Recherche Medicale, Philippe Fondation, and NIH grant AG15393.

The costs of publication of this article were defrayed in part by the payment of page charges. This article must therefore be hereby marked *advertisement* in accordance with 18 U.S.C. Section 1734 solely to indicate this fact.

We thank the personnel of the animal facility at Burnham Institute for Medical Research (La Jolla, CA) for excellent technical assistance; G. Salvesen and J.B. Denault for cyclin B, cyclin D3, Cdk2, Cdk4, Cip1/WAF1(p21), Kip1/p27 (p27), and Rb antibodies; and A.G. Carrion for technical assistance with real-time PCR.

References

1. Michalopoulos GK, DeFrances MC. Liver regeneration. Science 1997;276:60–6.
2. Mangnall D, Bird NC, Majeed AW. The molecular physiology of liver regeneration following partial hepatectomy. Liver Int 2003;23:124–38.
3. El-Serag HB. Hepatocellular carcinoma: an epidemiologic view. J Clin Gastroenterol 2002;35:S72–8.
4. Taub R. Liver regeneration 4: transcriptional control of liver regeneration. FASEB J 1996;10:413–27.
5. Fausto N. Liver regeneration. J Hepatol 2000;32:19–31.
6. Strey CW, Markiewski M, Mastellos D, et al. The proinflammatory mediators C3a and C5a are essential for liver regeneration. J Exp Med 2003;198:913–23.
7. Cressman DE, Greenbaum LE, DeAngelis RA, et al. Liver failure and defective hepatocyte regeneration in interleukin-6-deficient mice. Science 1996;274:1379–83.
8. Yamada Y, Kirillova I, Peschon JJ, Fausto N. Initiation of liver growth by tumor necrosis factor: deficient liver regeneration in mice lacking type I tumor necrosis factor receptor. Proc Natl Acad Sci U S A 1997;94:1441–6.
9. Classon M, Harlow E. The retinoblastoma tumour suppressor in development and cancer. Nat Rev Cancer 2002;2:910–7.
10. Xu Q, Reed JC. Bax inhibitor-1, a mammalian apoptosis suppressor identified by functional screening in yeast. Mol Cell 1998;1:337–46.
11. Bolduc N, Ouellet M, Pitre F, Brisson LF. Molecular characterization of two plant BI-1 homologues which suppress Bax-induced apoptosis in human 293 cells. Planta 2003;216:377–86.
12. Chae HJ, Kim HR, Xu C, et al. BI-1 regulates an apoptosis pathway linked to endoplasmic reticulum stress. Mol Cell 2004;15:355–66.
13. Grzmil M, Thelen P, Hemmerlein B, et al. Bax inhibitor-1 is overexpressed in prostate cancer and its specific down-regulation by RNA interference leads to cell death in human prostate carcinoma cells. Am J Pathol 2003;163:543–52.
14. Zhang BH, Hornsfield BP, Farrell GC. Chronic ethanol administration to rats decreases receptor-operated mobilization of intracellular ionic calcium in cultured hepatocytes and inhibits 1,4,5-inositol trisphosphate production: relevance to impaired liver regeneration. J Clin Invest 1996;98:1237–44.
15. Hesketh TR, Morris JD, Moore JP, Metcalfe JC. Ca^{2+} and pH responses to sequential additions of mitogens in single 3T3 fibroblasts: correlations with DNA synthesis. J Biol Chem 1988;263:11879–86.
16. Berridge MJ. Inositol trisphosphate and calcium signalling. Nature 1993;361:315–25.
17. Demaurex N, Distelhorst C. Cell biology. Apoptosis—the calcium connection. Science 2003;300:65–7.
18. Pinton P, Ferrari D, Magalhaes P, et al. Reduced loading of intracellular Ca(2+) stores and downregulation of capacitative Ca(2+) influx in Bcl-2-overexpressing cells. J Cell Biol 2000;148:857–62.
19. Baffy G, Miyashita T, Williamson JR, Reed JC. Apoptosis induced by withdrawal of interleukin-3 (IL-3) from an IL-3-dependent hematopoietic cell line is associated with repartitioning of intracellular calcium and is blocked by enforced Bcl-2 oncoprotein production. J Biol Chem 1993;268:6511–9.
20. Chen R, Valencia I, Zhong F, et al. Bcl-2 functionally interacts with inositol 1,4,5-trisphosphate receptors to regulate calcium release from the ER in response to inositol 1,4,5-trisphosphate. J Cell Biol 2004;166:193–203.
21. Scorrano L, Oakes SA, Opferman JT, et al. BAX and BAK regulation of endoplasmic reticulum Ca^{2+}: a control point for apoptosis. Science 2003;300:135–9.
22. Bonnefoy-Berard N, Aouacheria A, Verschelde C, Quemeneur L, Marcais A, Marvel J. Control of proliferation by Bcl-2 family members. Biochim Biophys Acta 2004;1644:159–68.
23. Vail ME, Chaisson ML, Thompson J, Fausto N. Bcl-2 expression delays hepatocyte cell cycle progression during liver regeneration. Oncogene 2002;21:1548–55.
24. Linette GP, Li Y, Roth K, Korsmeyer SJ. Cross talk between cell death and cell cycle progression: BCL-2 regulates NFAT-mediated activation. Proc Natl Acad Sci U S A 1996;93:9545–52.
25. O'Reilly LA, Huang DC, Strasser A. The cell death inhibitor Bcl-2 and its homologues influence control of cell cycle entry. EMBO J 1996;15:6979–90.
26. Brady HJ, Gil-Gomez G, Kirberg J, Berns AJ. Bax α perturbs T cell development and affects cell cycle entry of T cells. EMBO J 1996;15:6991–7001.
27. Higgins G, Anderson R. Experimental pathology of the liver. I. Restoration of the liver white rat following partial surgical removal. Arch Pathol 1931;12:186–202.
28. Berry MN, Friend DS. High-yield preparation of isolated rat liver parenchymal cells: a biochemical and fine structural study. J Cell Biol 1969;43:506–20.
29. Bailly-Maitre B, de Sousa G, Zucchini N, Gugenheim J, Boulukos KE, Rahmani R. Spontaneous apoptosis in primary cultures of human and rat hepatocytes: molecular mechanisms and regulation by dexamethasone. Cell Death Differ 2002;9:945–55.
30. Greenbaum LE, Li W, Cressman DE, et al. CCAAT enhancer-binding protein β is required for normal hepatocyte proliferation in mice after partial hepatectomy. J Clin Invest 1998;102:996–1007.
31. Dyson N. The regulation of E2F by pRB-family proteins. Genes Dev 1998;12:2245–62.
32. Dotto GP. p21(WAF1/Cip1): more than a break to the cell cycle? Biochim Biophys Acta 2000;1471:M43–56.
33. Nicou A, Serriere V, Prigent S, et al. Hypothalamic vasopressin release and hepatocyte Ca^{2+} signaling during liver regeneration: an interplay stimulating liver growth and bile flow. FASEB J 2003;17:1901–3.
34. Magnino F, St-Pierre M, Luthi M, Hilly M, Mauger JP, Dufour JF. Expression of intracellular calcium channels and pumps after partial hepatectomy in rat. Mol Cell Biol Res Commun 2000;3:374–9.
35. Diaz-Munoz M, Canedo-Merino R, Gutierrez-Salinas J, Hernandez-Munoz R. Modifications of intracellular calcium release channels and calcium mobilization following 70% hepatectomy. Arch Biochem Biophys 1998;349:105–12.
36. Kahl CR, Means AR. Regulation of cell cycle progression by calcium/calmodulin-dependent pathways. Endocr Rev 2003;24:719–36.
37. Rao A, Luo C, Hogan PG. Transcription factors of the NFAT family: regulation and function. Annu Rev Immunol 1997;15:707–47.
38. Lin JX, Vilcek J. Tumor necrosis factor and interleukin-1 cause a rapid and transient stimulation of c-fos and c-myc mRNA levels in human fibroblasts. J Biol Chem 1987;262:11908–11.
39. Jenab S, Quinones-Jenab V. The effects of interleukin-6, leukemia inhibitory factor and interferon-γ on STAT DNA binding and c-fos mRNA levels in cortical astrocytes and C6 glioma cells. Neuroendocrinol Lett 2002;23:325–8.
40. Schuringa JJ, Timmer H, Luttickhuizen D, Vellenga E, Kruijer W. c-Jun and c-Fos cooperate with STAT3 in IL-6-induced transactivation of the IL-6 response element (IRE). Cytokine 2001;14:78–87.
41. Vail ME, Pierce RH, Fausto N. Bcl-2 delays and alters hepatic carcinogenesis induced by transforming growth factor α. Cancer Res 2001;61:594–601.
42. Truchet I, Jozan S, Guerrin M, Mazzolini L, Vidal S, Valette A. Interconnections between E2-dependent regulation of cell cycle progression and apoptosis in MCF-7 tumors growing on nude mice. Exp Cell Res 2000;254:241–8.
43. Kuwana T, Newmeyer DD. Bcl-2-family proteins and the role of mitochondria in apoptosis. Curr Opin Cell Biol 2003;15:691–9.
44. Ferri KF, Kroemer G. Organelle-specific initiation of cell death pathways. Nat Cell Biol 2001;3:E255–63.
45. Novotny V, Prieschl EE, Csonga R, Fabjani G, Baumruker T. Nrf1 in a complex with fosB, c-jun, junD, and ATF2 forms the AP1 component at the TNF α promoter in stimulated mast cells. Nucleic Acids Res 1998;26:5480–5.
46. Morse D, Pischke SE, Zhou Z, et al. Suppression of inflammatory cytokine production by carbon monoxide involves the JNK pathway and AP-1. J Biol Chem 2003;278:36993–8.
47. de la Coste A, Fabre M, McDonell N, et al. Differential protective effects of Bcl-xL and Bcl-2 on apoptotic liver injury in transgenic mice. Am J Physiol 1999;277:G702–8.
48. de La Coste A, Mignon A, Fabre M, et al. Paradoxical inhibition of c-myc-induced carcinogenesis by Bcl-2 in transgenic mice. Cancer Res 1999;59:5017–22.
49. Tanaka R, Ishiyama T, Uchihara T, et al. Expression of the Bax inhibitor-1 gene in pulmonary adenocarcinoma. Cancer 2006;106:648–53.
50. Grzmil M, Kaulfuss S, Thelen P, et al. Expression and functional analysis of Bax inhibitor-1 in human breast cancer cells. J Pathol 2006;208:340–9.

Mice Lacking *bi-1* Gene Show Accelerated Liver Regeneration

Béatrice Bailly-Maitre, Emilie Bard-Chapeau, Fréderic Luciano, et al.

Cancer Res 2007;67:1442-1450.